Temperature Dependence of Benzyl Alcohol- and 8-Anilinonaphthalene-1-sulfonate-Induced Aggregation of Recombinant Human Interleukin-1 Receptor Antagonist[†]

Shouvik Roy,[‡] Derrick Katayama,[‡] Aichun Dong,[§] Bruce A. Kerwin,[||] Theodore W. Randolph,[⊥] and John F. Carpenter*,[‡]

Center for Pharmaceutical Biotechnology, Department of Pharmaceutical Sciences, University of Colorado Health Sciences Center, Denver, Colorado 80262, Department of Chemistry and Biochemistry, University of Northern Colorado, Greeley, Colorado 80639, Department of Pharmaceutics, Amgen Inc., Thousand Oaks, California 91320, and Department of Chemical Engineering, University of Colorado, Boulder, Colorado 80309

ABSTRACT: The critical role played by temperature in ligand-induced protein aggregation was investigated. Recombinant human interleukin-1 receptor antagonist (rhIL-1ra) and the ligands benzyl alcohol and 8-anilinonaphthalene-1-sulfonate (ANS) were used. We investigated aggregation kinetics and the conformation and cysteine reactivity of rhIL-1ra in buffer alone or in the presence of 0.9% (w/v) benzyl alcohol or 4.2 or 21 mM ANS at 25 and 37 °C. In buffer, protein aggregation was not detected at 25 °C but occurred at 37 °C. At 25 °C, neither benzyl alcohol nor 4.2 mM ANS enhanced aggregation. However, at 37 °C, both compounds greatly accelerated protein aggregation. With 21 mM ANS, rhIL-1ra aggregation was accelerated at both temperatures, but the effect was more pronounced at 37 °C than at 25 °C. Increasing the temperature from 25 to 37 °C caused a minor perturbation in the tertiary structure of rhIL-1ra in buffer but no detectable alteration in secondary structure. Benzyl alcohol enhanced the tertiary structural perturbation at 37 °C, but the secondary structure was not affected by the ligand. The reactivity of buried free cysteines of rhIL-1ra was enhanced by benzyl alcohol at 37 °C but not at 25 °C, consistent with the structural results. Isothermal titration calorimetry documented that the interaction of benzyl alcohol with rhIL-1ra was hydrophobic and that the degree of hydrophobic interactions increased with temperature. At 25 °C, the interaction of ANS with rhIL-1ra was electrostatic, but at 37 °C, both electrostatic and hydrophobic interactions were important. Taken together, our results support the conclusion that benzyl alcohol and ANS interact hydrophobically with partially unfolded aggregation-prone protein molecules, resulting in temperature-dependent increases in their levels and acceleration of protein aggregation.

Aggregation of proteins is a major problem in certain human disease states and development of biopharmaceuticals. Aggregation of proteins to form insoluble fibrils has been implicated in several diseases, including Alzheimer's, Parkinson's, and Huntington's diseases (1–3). Aggregation of therapeutic proteins can arise during any phase of downstream processing (e.g., purification, filtration, and storage of bulk drug substance), and during shipping, storage, and administration of the final drug formulation to patients. The administration of products containing non-native aggregates can cause adverse reaction in patients (4–6). Thus, there is great need to understand the mechanisms of protein aggregation and how solution conditions govern this process.

Non-native protein aggregates are formed from partially unfolded protein molecules which have more solvent-exposed hydrophobic surfaces than the most compact species within the native state ensemble (7–9). A rational strategy for inhibiting aggregation employs ligands that bind strongly with the most compact native state species (10, 11), which according to the Wyman linkage function will shift the equilibrium toward this species (12). The resulting reduction in concentration of partially unfolded protein molecules reduces the rate of aggregation. For example, Kelly and colleagues have found that compounds that bind to the native tetramer of transthyretin greatly reduce the aggregation rate of this protein (13). Likewise, for some therapeutic protein products, ligands that bind specifically with the native state have been used to minimize aggregation. For instance, binding of polyanions to the native state of acidic fibroblast growth factor stabilizes the protein against aggregation (14, 15). In contrast, sometimes ligand binding can promote protein aggregation. For example, with immunoglobulin light chain variable domains, it has been found that Congo red can interact most favorably with partially unfolded protein molecules, resulting in an increase in their concentration and

* To whom correspondence should be addressed: Center for Pharmaceutical Biotechnology, University of Colorado Health Sciences Center, 4200 E. 9th Ave., Denver, CO 80262. Telephone: (303) 315-6075. Fax: (303) 315-6281. E-mail: John.Carpenter@uchsc.edu.
‡ University of Colorado Health Sciences Center.
§ University of Northern Colorado.
|| Amgen Inc.
⊥ University of Colorado.

a concomitant increase in aggregation rate (*16*). Nucleic acids have also been shown to enhance oligomerization and increase the β-sheet content of cellular prion proteins (*17*). Similarly, the antimicrobial preservative benzyl alcohol accelerates aggregation by binding to and populating partially unfolded species of recombinant human interleukin-1 receptor antagonist (*18*). Thus, ultimately the effect of ligand binding on protein stability depends on the species within the protein molecular population to which the ligand binds most.

A critically important, but often ignored, factor that influences the effect of protein−ligand interactions on protein stability is temperature. For example, in some studies, inhibitors of amyloid fibril formation have been tested at room temperature instead of physiological temperature (*19*). Conversely, with therapeutic proteins, the effects of ligands on aggregation are often studied at elevated temperatures, to shorten the time needed to screen formulation components, even though the commercial products are usually stored at 4−8 °C (*20*). In both cases, the results can be misleading, especially for ligands that interact hydrophobically with proteins and thus are more strongly interacting at elevated temperatures (*21*). For example, alcohols reduce the free energy of protein unfolding at elevated temperatures, yet they can be protein stabilizers at low temperatures (*22*). In the former case, alcohols interact most strongly with, and favor, the denatured state through hydrophobic interactions. In contrast, at low temperatures, alcohols are preferentially excluded from the surface of the protein molecules, resulting in a shift in the equilibrium toward the more compact native state and away from the denatured state (*22*).

To address the issue of temperature-dependent effects of ligands on protein aggregation, we have chosen to study two ligands of different classes, both of which are widely used but for different purposes. The ligands were benzyl alcohol and 8-anilinonaphthalene-1-sulfonate (ANS),[1] which are known to interact with proteins hydrophobically (*23*, *24*). As a model therapeutic protein, we chose recombinant human interleukin-1 receptor antagonist because the effects of benzyl alcohol and other solution additives on its aggregation and stability have been studied in detail (*18*, *25*−*27*), but the temperature dependency of these effects has not been investigated.

Benzyl alcohol is often used at 0.9% (w/v) as an antimicrobial preservative in multidose therapeutic products (*28*) but is limited in its use with therapeutic proteins because of its capacity to greatly accelerate protein aggregation (*18*, *29*, *30*). Recently, it was shown that benzyl alcohol induces rapid aggregation of rhIL-1ra at 37 °C by interacting with protein molecules hydrophobically, thus increasing the levels of aggregation-prone partially unfolded species in the protein molecular population (*18*). We hypothesize that benzyl alcohol-induced aggregation will be attenuated at lower temperatures, such as room temperature which is often used for storage of multidose therapeutic protein products. Furthermore, we predict that the slowed aggregation will be due

to a reduction in the levels of partially unfolded protein molecules populated in the presence of benzyl alcohol.

ANS is a commonly used fluorescent probe used to detect partially unfolded protein molecules (*23*, *31*, *32*). ANS has a negatively charged sulfonate group and a nonpolar anilinonaphthalene group. Some studies have shown that ANS interacts with proteins predominantly through the formation of ion pairs between the negatively charged sulfonate group and positive charges on proteins (*33*−*35*). In these studies, the proteins under investigation were conformationally expanded using acidic conditions and thus possessed a highly positive net charge. Interaction with ANS was consequently electrostatic. However, under neutral and alkaline conditions, and depending on the degree of hydrophobic surfaces present on the protein, interactions with ANS can be dominated by hydrophobic interactions (*36*−*39*).

Although ANS is often considered to be a "probe" for detecting partially unfolded protein molecules in dilute aqueous solutions, according to the Wyman linkage function preferential binding of ANS with these species will increase their levels (*18*). For example, it has been found in protein refolding studies that ANS can increase the levels of partially folded protein species and increase their lifetimes (*40*, *41*). At the low concentrations of protein usually used for the fluorescence measurement of ANS binding, ANS-induced increases in the level of partially unfolded protein molecules probably rarely result in aggregation. However, in a recent study, micromolar amounts of various naphthalene sulfonates were found to stabilize low-molecular weight oligomers implicated in Alzheimer's disease (*42*). Also, with the dimeric form of ANS, bis-ANS, it has been found that with sufficiently high bis-ANS concentrations, the increased levels of partially unfolded molecules fostered protein oligomerization (*42*). We hypothesize that the same effect will be seen with ANS and rhIL-1ra and that the acceleration of aggregation will be enhanced at elevated temperatures due to hydrophobic interactions.

To test our hypotheses, we have quantified the effects of benzyl alcohol and ANS on aggregation of rhIL-1ra in aqueous solution at 25 and 37 °C. In addition, we have determined the temperature-dependent effects of benzyl alcohol and ANS on the secondary and tertiary structures of the protein. And with isothermal titration calorimetry (ITC), we have characterized the thermodynamics of interactions of benzyl alcohol and ANS with the protein. Interference of ANS with some of the spectroscopic methods employed for structural studies precluded an evaluation of the effects of this ligand on the tertiary structure of rhIL-1ra.

MATERIALS AND METHODS

Materials. rhIL-1ra (>98% pure, molecular mass = 17 kDa) was a generous gift from Amgen Inc. and was obtained as a 220 mg/mL stock solution in 10 mM sodium citrate buffer and 140 mM sodium chloride (pH 6.5 at room temperature). The stock protein solution was frozen and stored at −80 °C and then thawed and reformulated as needed. Potassium phosphate, NaCl, benzyl alcohol, 4-chloro-7-nitrobenzen-2-oxa-1,3-diazole (NbdCl), and 8-anilinonaphthalene-1-sulfonate (ANS) were purchased from Sigma Chemical Co. (St. Louis, MO).

Aggregation of rhIL-1ra during Incubation in Aqueous Solution. The effect of temperature on benzyl alcohol- and

---

[1] Abbreviations: rhIL-1ra, recombinant human interleukin-1 receptor antagonist; ANS, 8-anilinonaphthalene-1-sulfonate; ITC, isothermal titration calorimetry; NbdCl, 4-chloro-7-nitrobenzen-2-oxa-1,3-diazole; SEC, size-exclusion chromatography; IR, infrared; UV CD, ultraviolet circular dichroism.

ANS-induced aggregation of rhIL-1ra was investigated by incubating the protein at 25 or 37 °C for 7 days in "buffer" [10 mM potassium phosphate buffer (pH 7) containing 140 mM NaCl]. rhIL-1ra (70 mg/mL, 4.2 mM) was incubated in the presence of 0.9% (w/v) benzyl alcohol, 4.2 or 21 mM ANS, or no added ligand. For benzyl alcohol, 0.9% (w/v) represents the antimicrobial concentration generally used in protein formulations (20). In fluorescence measurements, to detect partially unfolded states of proteins, ANS is generally used at ANS:protein molar ratios of 10−70 (42−46), but at concentrations sufficiently low that the "inner filter" effect in fluorescence is not introduced. Thus, when ANS is used as a probe for partially unfolded protein molecules, typically micromolar concentrations are used. Because our purpose was to employ this ligand to induce protein aggregation, we initially used ANS at a concentration of 21 mM, which is equivalent to an ANS:rhIL-1ra molar ratio of 5. At this ANS concentration, the aggregation of rhIL-1ra at both 25 and 37 °C was rapid. Therefore, to resolve the effect of temperature on ANS-induced protein aggregation more distinctly, the studies described above were also performed at a lower ANS concentration of 4.2 mM.

Samples of rhIL-1ra solutions were incubated as 250 μL aliquots in sealed 500 μL Eppendorf tubes in 25 and 37 °C water baths for 7 days. For each time point, separate tubes in triplicate were used. At each time point, the tubes were removed from the water bath and centrifuged at 13500*g* (4 °C) for 10 min to pellet any insoluble precipitates. A 10 μL aliquot of the supernatant was carefully removed and diluted 50-fold with buffer devoid of any ligand. A 20 μL aliquot was then used for analysis by size exclusion chromatography (SEC) to quantify levels of soluble protein. SEC analysis was performed using a Tosohaas TSK 3000SW gel filtration column connected to a Hewlett-Packard 1090 chromatography system. A filtered and degassed mobile phase consisting of 10 mM potassium phosphate and 140 mM NaCl (pH 7.0) was used at a flow rate of 0.6 mL/min. Chromatogram peak areas were used to quantify soluble protein by UV detection at 280 nm. The average monomer peak areas of freshly prepared rhIL-1ra samples in each solution served as the controls. The fraction of soluble protein remaining was determined by dividing the sample peak area by the average of the control samples. No soluble aggregates were detected in any of the samples (data not shown).

Precipitates of rhIL-1ra formed during incubation of the protein in buffer alone and in the presence of the ligands were collected by centrifugation at the end of 7 days and resuspended in buffer devoid of any ligand. This wash procedure was repeated twice, and the infrared spectra of the precipitated protein were collected using a Bomem-Prota infrared (IR) spectrometer (MB series). A sample cell consisting of a CaF_2 window with a fixed path length of 6 μm was used for the measurements. An IR spectrum of native rhIL-1ra in solution was collected by placing the sample in a liquid IR cell with CaF_2 windows separated by a 6 μm Mylar spacer (Chemplex Industries). Sample spectra were collected with 128 scans in the single-beam data collection mode with a resolution of 4 cm^{-1}. Spectra for buffer blanks were collected under identical conditions. The spectra were converted into absorbance signals and processed to subtract the signal from water as previously described (47). The resulting area-normalized second-derivative spectra for the

native and precipitated protein were overlaid to detect differences in the secondary structure of rhIL-1ra.

Secondary Structural Studies. The effect of temperature on the secondary structure of rhIL-1ra in buffer alone and in the presence of benzyl alcohol or ANS was determined. Far-UV circular dichroism (far-UV CD) was used for rhIL-1ra in buffer alone. It was not possible to determine the effects of 0.9% benzyl alcohol or 4.2 or 21 mM ANS on the secondary structure of rhIL-1ra using far-UV CD, because of the strong absorbance of these compounds. Far-UV CD spectra for rhIL-1ra in buffer alone were collected at a protein concentration of 0.1 mg/mL using a 1 mm path length quartz cell, as a function of temperature. The spectra were collected from 260 to 200 nm using an Aviv-62 DS circular dichroism spectrometer equipped with a Peltier temperature control unit. Data were collected every 0.25 nm, with an averaging time of 5 s, and a 1.5 nm bandwidth.

IR spectroscopy was used to study protein samples (15 mg/mL) in buffer alone and in the presence of 0.9% (w/v) benzyl alcohol or 4.2 or 21 mM ANS. At the higher ANS concentration, the sample aggregated before the first IR spectrum could be acquired. IR spectra were collected by placing samples in a heatable liquid IR cell (Graseby Specac) with CaF_2 windows and a 6 μm Mylar spacer. IR spectra were collected under identical conditions for each sample and its corresponding buffer. For each spectrum, a 128-scan interferogram was collected in a single-beam mode with a 4 cm^{-1} resolution. Measurements were conducted at 25 and 37 °C, with the sample temperature controlled within 0.5 °C (recorded with a T-type thermocouple placed within a depression in the CaF_2 window) using a custom-built Peltier temperature controller. The spectra were then processed as described above.

In addition, to follow in real time changes in rhIL-1ra secondary structure during ligand-induced aggregation, IR spectra were also collected for rhIL-1ra samples for 2 h at 25 and 37 °C as described above, but with acquisition of 64-scan interferograms. Using 64 scans allowed early time point spectra to be collected so that the time-dependent structural transition could be assessed for faster aggregating samples.

Tertiary Structural Studies. Near-UV CD spectroscopy was used to detect changes in the tertiary structure of rhIL-1ra in buffer alone and in the presence of benzyl alcohol. The tertiary structure of rhIL-1ra in the presence of ANS could not be determined by either near-UV CD or the alternative methods of second-derivative absorbance or intrinsic fluorescence spectroscopy due to strong interference of ANS with the protein signal at concentrations used in the study.

Near-UV CD spectra of buffer solutions containing 1 mg/mL rhIL-1ra were collected from 340 to 250 nm with a bandwidth of 1 nm, using a 1 cm path length quartz cell and the instrumentation described above for the far-UV CD measurements. For rhIL-1ra in buffer alone, changes in tertiary structure were detected by monitoring changes in the signal intensity of phenylalanine (250−268 nm), tyrosine, and tryptophan residues (between 280 and 295 nm) (48). Spectra for samples with 0.9% (w/v) benzyl alcohol were truncated at 270 nm due to the strong absorbance of benzyl alcohol below this wavelength. To improve the signal quality, each spectrum was recorded as the average of three separate scans.

Reactivity of rhIL-1ra Cysteines. The reactivity of free thiol groups of rhIL-1ra with NbdCl was used to evaluate the conformational dynamics of the protein (26, 49) in buffer alone and in the presence of benzyl alcohol. This method could not be used with ANS because of its absorbance at 420 nm, the wavelength at which the reaction of NbdCl with thiol is monitored. In a previous application of this method to the study of rhIL-1ra (26), NbdCl was dissolved in ethanol at a stock concentration of 16.4 mg/mL (near the limit of solubility in this solvent). A 3 μL aliquot of the stock solution was added to 1 mL of the protein solution (26). Because this study investigates the effects of benzyl alcohol on the conformation and stability of rhIL-1ra, we did not want to include a second alcohol, which could affect these parameters, in the reaction mixture. Therefore, we prepared the NbdCl stock solution in chloroform because the reagent has a higher solubility (50 mg/mL) in this solvent than in ethanol. Using a stock solution of NbdCl in chloroform at 50 mg/mL, we could reduce the amount of organic solvent to be added to the reaction mixture to 0.6 μL/mL of protein solution.

The reaction of NbdCl (stock concentration of 50 mg/mL in chloroform) with free thiol groups of rhIL-1ra (concentration of 0.1 mg/mL) was initiated by pipetting 0.6 μL of the stock NbdCl into 1 mL of the protein solution. As a control for a potential direct effect of temperature and 0.9% (w/v) benzyl alcohol on thiol reactivity, NbdCl was reacted with reduced glutathione (final concentration of 1.5 μg/mL) under the conditions described above. Benzyl alcohol had no direct effect on the reactivity of free reduced glutathione in solution with NbdCl at any of the temperatures that were studied (data not shown).

The reaction of NbdCl with free cysteines in rhIL-1ra was followed by monitoring the absorbance at 420 nm until the absorbance reached a plateau (after ca. 90 min) indicative of completion of the reaction. The absorbance values measured for the different samples were converted into the fraction of reaction completed using the relationship $Y_{fraction} = (Y_t - Y_{initial})/(Y_{complete} - Y_{initial})$, where Y_t is the absorbance measured at any time (t), $Y_{initial}$ is the absorbance value immediately after the reaction is initiated, and $Y_{complete}$ is the absorbance value after saturation has been reached (50). Because of the biphasic nature of the reaction curves, curve fitting was used to obtain rate constants for the fast and slow reacting groups based on the following equation, using Igor Pro 4.0.6.1 WaveMetrics, Inc., software

$$f(x) = (1 - 1/k_{fast}) \times \exp(-k_{slow}x)$$

To determine the activation energies for the slow and fast reacting cysteines of rhIL-1ra, the experiments were performed over a temperature range from 25 to 42 °C. An Arrhenius plot was subsequently constructed by plotting the natural logarithm of the slow and fast rates against the inverse of the absolute temperature (data not shown). The slope of the straight line thus obtained from this plot was used to determine the activation energy (E_a) using the universal gas constant (R = 8.31 J mol^{-1} K^{-1}).

Thermal Stability of rhIL-1ra. The thermal stability of rhIL-1ra in buffer alone and in the presence of 0.9% (w/v) benzyl alcohol was evaluated using second-derivative UV absorbance spectroscopy, near-UV CD spectroscopy, and

differential scanning calorimetry (DSC). Due to interference by ANS with the optical methods, the thermostability of rhIL-1ra in the presence of 4.2 or 21 mM ANS was determined by DSC.

For UV absorbance spectroscopy, an Agilent (Palo Alto, CA) 8453 UV−visible spectrophotometer, equipped with a temperature controller unit, was used. A 3 mL sample with 0.1 mg/mL rhIL-1ra was placed in a sealed 1 cm path length quartz cuvette and heated from 15 to 75 °C at 1.5 °C intervals. The sample was stirred at 150 rpm. A 3 min equilibration was allowed before each spectrum was collected between 200 and 500 nm, with a 1 nm interval and an integration time of 10 s. Second-derivative spectra were calculated using a five-point data filter and a three-degree Savitzky−Golay polynomial and subsequently fitted to a cubic function, with 32 interpolated points per raw data point (18). The second-derivative spectrum of native rhIL-1ra had two maxima centered around 287 and 295 nm and two minima at 283 and 290.5 nm attributed to signals from Trp/Tyr and Trp, respectively. To assess the thermostability of rhIL-1ra in buffer alone and in the presence of benzyl alcohol, a change in the tryptophan peak position (290.5 nm), the tyrosine/tryptophan peak intensity (283 nm), and the a/b ratio were monitored as a function of temperature. The optical density at 350 nm, indicating protein aggregation (18), was also monitored. To ascertain the potential of a direct effect of temperature and benzyl alcohol on the peak positions and a/b ratio of the aromatic acids, spectra of a mixture of *N*-acetyltyrosinamide and *N*-acetyltryptophanamide were obtained, with the same tyrosine:tryptophan molar ratio as in rhIL-1ra.

Thermal stability was examined with near-UV CD by heating the samples (1 mg/mL rhIL-1ra) between 15 and 75 °C at 1 °C intervals and monitoring the signal intensity at 281 nm. Data were collected with an averaging time of 5 s and with an equilibration for 0.5 min at each temperature.

Thermal stability was examined with DSC using a MCS microcalorimeter from Microcal (Northhampton, MA) at a rhIL-1ra concentration of 1 mg/mL. Samples were prepared in buffer alone, 0.9% (w/v) benzyl alcohol, or 4.2 or 21 mM ANS. Samples were heated between 15 and 90 °C at a rate of 90 °C/h, and thermal data were acquired. To check for reversibility, after the samples were cooled to 15 °C, a second heating scan was performed.

Isothermal Titration Calorimetry (ITC) Studies. The thermodynamics of the interaction of benzyl alcohol and 4.2 mM ANS with rhIL-1ra at 25 and 37 °C were characterized using an isothermal titration microcalorimeter (VP-ITC, Microcal Inc.) (51). The samples were thoroughly degassed before each titration for approximately 8 min. With 21 mM ANS, the protein aggregated even at 25 °C, precluding ITC measurements.

Experiments with benzyl alcohol were performed by placing a solution of 50 mg/mL rhIL-1ra (3 mM) in buffer in the sample cell and 1.5% benzyl alcohol (145 mM) in buffer in the titrant syringe (18). The sample in the cell was stirred by the syringe at 350 rpm. A total of 28 injections were made, with 5 μL of titrant injected each for the first six injections, followed by 10 μL each for the remaining ones. The titrant was delivered over 6.5 s with 180 s intervals between each injection to allow equilibration. The data were collected automatically and subsequently analyzed by Origin

from Microcal Inc. Before the curve fitting process, a background titration consisting of the identical benzyl alcohol solution but with only buffer in the sample cell was subtracted from each experimental titration to account for the heat of dilution (*51*). The data were best described by a nonlinear least-squares fit of the one-site binding model.

Binding of ANS to rhIL-1ra was assessed with 4.2 mM ligand in the syringe and 12.25 mg/mL (0.735 mM) rhIL-1ra in the sample cell. The injection procedure was the same as that described for benzyl alcohol but with 28 identical injections of 10 μL each. The heat of dilution of ANS with buffer alone was negligible as also reported by others (*36*) and was subtracted from the heat of titration of the samples. At 25 °C, the data were best fit by a one-site binding model, whereas at 37 °C, a two-site binding model provided a better fit. A "one-site" or "two-site" model refers to a model in which one or two types of binding sites, respectively, are present on the protein, each of which can contain multiple binding sites with equal affinity for the ligand.

From the unconstrained fitting to the plot of the heat evolved per mole of titrant injected versus the molar ratio of benzyl alcohol or ANS to rhIL-1ra, the binding stoichiometry (n), the binding enthalpy (ΔH), and the dissociation constants (K_d) were determined. The Gibbs free energy of binding (ΔG) was calculated as $-RT \ln(1/K_d)$. The change in the entropy of binding (ΔS) was calculated as ($\Delta H - \Delta G$)/T.

RESULTS

Temperature Dependence of Benzyl Alcohol- and ANS-Induced Aggregation of rhIL-1ra. Aggregation of rhIL-1ra was investigated by incubating the protein solutions at 25 and 37 °C. At 25 °C, only a few percent of the protein aggregated in buffer alone, in 0.9% benzyl alcohol, or in 4.2 mM ANS during the 7 day incubation (Figure 1A,B), and the amount of aggregation was not statistically significantly different between these solutions. At 37 °C, although there was aggregation of protein in buffer alone, in the presence of benzyl alcohol or 4.2 mM ANS a much greater rate of aggregation was measured. For example, at 37 °C, more than 70 and 90% of rhIL-1ra aggregated within the first 2 days in the presence of 4.2 mM ANS and benzyl alcohol, respectively, compared to a less than 20% loss in monomer levels for the protein in buffer alone. These results strongly support our hypothesis and, furthermore, provide a clear example of how results for ligand-induced aggregation of proteins at elevated temperature may not accurately predict the relative effect of the given ligand on aggregation at lower temperatures.

Aggregation of rhIL-1ra was greatly accelerated in the presence of 21 mM ANS, with complete aggregation occurring within 6 and 2 hours at 25 and 37 °C, respectively (Figure 1B). Thus, in further support of our hypothesis, induction of aggregation by 21 mM ANS was also enhanced at higher temperatures.

Changes in Secondary Structure of rhIL-1ra during Aggregation. The insoluble aggregates present in samples at the end of the 7 day incubation were collected and characterized by IR spectroscopy (Figure 2A,B). The IR spectra of the aggregated protein samples reflected a large proportion of intermolecular β-sheet as indicated by strong
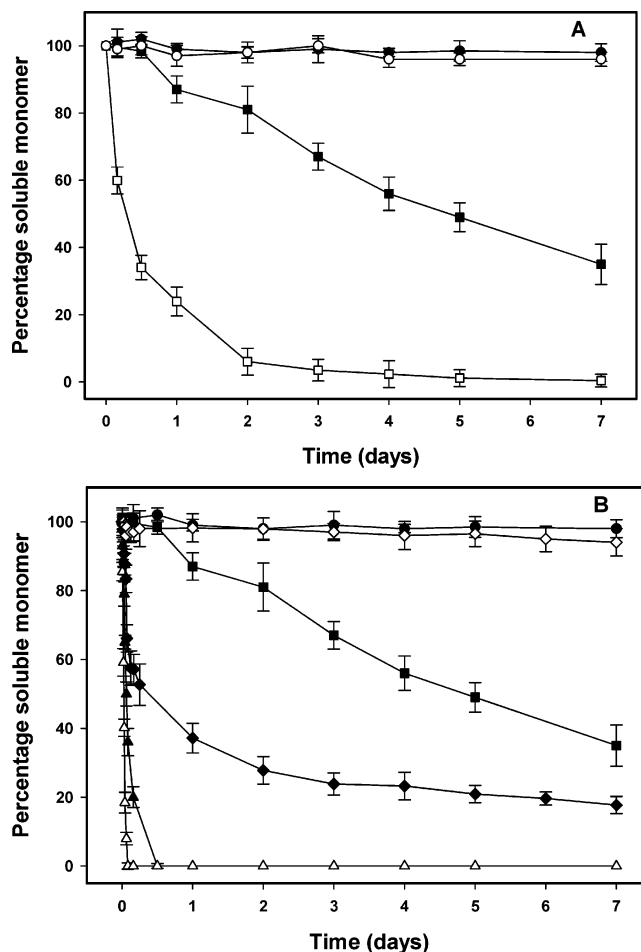

FIGURE 1: Percentage of soluble monomer of rhIL-1ra remaining in solution during incubation of rhIL-1ra at 25 and 37 °C for 7 days in buffer alone and in the presence of (A) benzyl alcohol or (B) ANS: rhIL-1ra in buffer alone at 25 °C (●), rhIL-1ra with benzyl alcohol at 25 °C (○), rhIL-1ra in buffer alone at 37 °C (■), rhIL-1ra with benzyl alcohol at 37 °C (□), rhIL-1ra with 4.2 mM ANS at 25 °C (◇), rhIL-1ra with 4.2 mM ANS at 37 °C (◆), rhIL-1ra with 21 mM ANS at 25 °C (▲), and rhIL-1ra with 21 mM ANS at 37 °C (△). Error bars indicate the standard deviation for triplicate samples.

bands at 1623 and 1693 cm^{-1} (*47*). In contrast, intramolecular β-sheet bands at 1642 and 1689 cm^{-1} are dominant in the spectrum of the native control sample and consistent with the high-resolution structure of this protein obtained via NMR spectroscopy (*52, 53*). These results document that aggregation and precipitation of rhIL-1ra resulted in gross perturbation of the protein's secondary structure.

To determine the time-dependent changes in secondary structure of rhIL-1ra during aggregation, real-time infrared spectra were acquired during 2 h incubations at 25 and 37 °C. At 25 °C, for the protein in buffer alone or with 0.9% (w/v) benzyl alcohol or 4.2 mM ANS, no change in the IR spectra could be detected for the 2 h period (data not shown). Similar observations were made for rhIL-1ra in buffer alone at 37 °C (data not shown). However, at 37 °C with 0.9% (w/v) benzyl alcohol or 4.2 mM ANS, there was a time-dependent decrease in the intensity of the native β-sheet band that was concomitant with an increase in the intensity of the intermolecular β-sheet band at 1627–1630 cm^{-1} (Figure 3A,B) (*54, 55*). Additionally, the band at 1689 cm^{-1} for these samples shifted to higher wavenumbers characteristic of
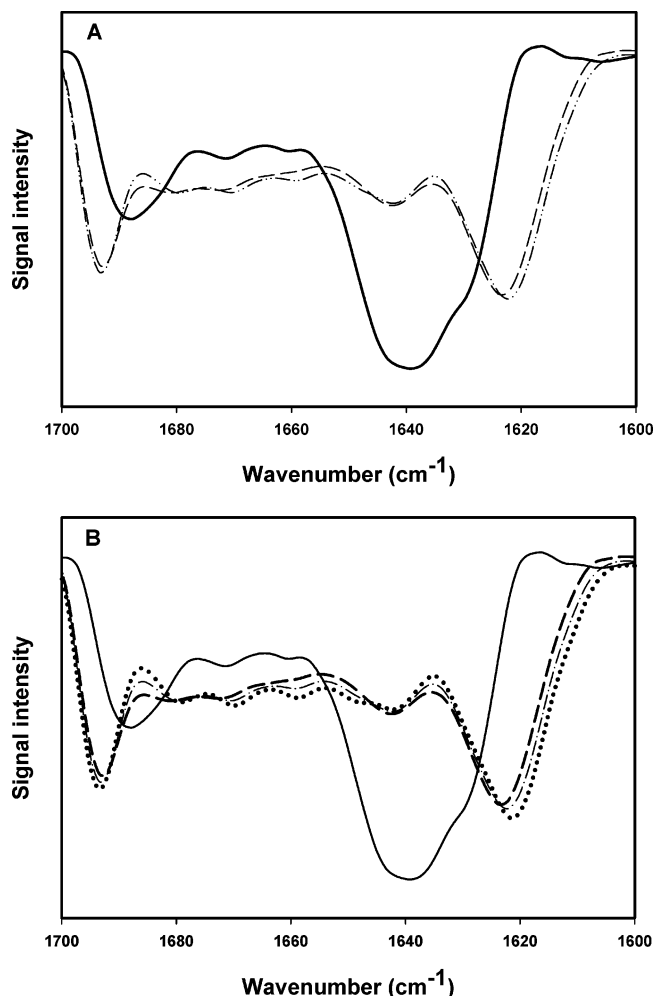
FIGURE 2: Second-derivative IR spectra of native rhIL-1ra in solution and protein precipitates at the end of the incubation obtained (A) in buffer alone or 0.9% (w/v) benzyl alcohol or (B) in 4.2 or 21 mM ANS: rhIL-1ra in aqueous solution (—), precipitate in buffer alone at 37 °C (− − −), precipitate in buffer and benzyl alcohol at 37 °C (−··−), precipitate in buffer and 4.2 mM ANS at 37 °C (− − −), precipitate in buffer and 21 mM ANS at 25 °C (−·−), and precipitate in buffer and 21 mM ANS at 37 °C (···).

intermolecular β-sheet formation (*52*). In the presence of 21 mM ANS, there was rapid aggregation of rhIL-1ra even at 25 °C (Figure 3C). At 37 °C, the conversion of native protein into aggregate was so rapid that within the first few minutes of monitoring the protein's infrared spectra, the band for the intermolecular β-sheet was dominant (Figure 3D).

The real-time IR measurements were not able to resolve any secondary structural changes in rhIL-1ra before it aggregated. The two isosbestic points at 1630 and 1650 cm^{-1} (e.g., Figure 3A) indicate that there was an apparent two-state structural transition from the native to the aggregated state (*54*, *55*). Thus, aggregation of rhIL-1ra could occur via a partially unfolded intermediate (*18*, *25*) with a secondary structure indistinguishable from that of the native protein. It is also possible that with the low sensitivity of the IR data, even if an intermediate is present as 10−20% of the population, its detection may be difficult.

Effects of Temperature and Ligands on rhIL-1ra Secondary Structure Prior to Aggregation. The far-UV CD and infrared spectra of rhIL-1ra in buffer alone were studied at 25 and 37 °C, to determine if secondary structural changes in the

protein arose prior to protein aggregation. In the presence of the benzyl alcohol or ANS, this was done by IR spectroscopy only. For the protein in buffer alone, the negative signal at around 205 nm in the far-UV CD spectra (Figure 4A) and the strong bands at 1642 and 1689 cm^{-1} (Figure 4B) in the IR spectra are consistent with the predominant antiparallel β-sheet secondary structure of native rhIL-1ra (*47*, *52*, *53*). The far-UV CD spectra of the protein at 25 and 37 °C were indistinguishable (Figure 4A). In the IR spectra, there is a small increase in the intensity of the major β-sheet band at 1642 cm^{-1} at 37 °C relative to that seen at 25 °C. Coupled with the far-UV CD results, the IR spectra indicate that the overall percentages of secondary structural elements were not altered in rhIL-1ra when the temperature was increased from 25 to 37 °C, but there were minor alterations in the microenvironments of the β-sheet residues.

In the presence of ANS or benzyl alcohol, far-UV CD spectra of rhIL-1ra could not be acquired due to the strong signal of the ligands in this spectral range (*18*, *30*). In 0.9% (w/v) benzyl alcohol, the IR spectrum of rhIL-1ra at 25 °C was almost identical to that for the protein in buffer alone, evidence that the secondary structure of the protein is not altered detectably by the alcohol at this temperature (Figure 5A). At 37 °C, there were minor changes in the β-sheet bands at 1642 and ~1690 cm^{-1}, indicating that small changes in the protein's secondary structure occurred in the presence of 0.9% (w/v) benzyl alcohol. At 25 °C in 4.2 mM ANS, the protein's IR spectrum was almost identical to that for the protein in buffer alone (Figure 5A). However, at 37 °C, 4.2 mM ANS caused minor alterations in the protein's secondary structure (Figure 5B). In 21 mM ANS, the protein aggregated at both 25 and 37 °C within the time needed for sample mixing, IR cell loading, and spectral acquisition (approximately 10 min), as evidenced by bands in the IR spectra for protein aggregates (1627−1630 cm^{-1}) (Figure 5A,B).

Effects of Temperature and Ligands on rhIL-1ra Tertiary Structure Prior to Aggregation. The effects of temperature on rhIL-1ra tertiary structure in buffer alone and in 0.9% (w/v) benzyl alcohol were investigated using near-UV CD. Spectra of the protein in ANS could not be acquired due to the strong signal of the ligand in this spectral range. In buffer alone, an increase in temperature from 25 to 37 °C caused a small but significant alteration in the near-UV CD spectrum of rhIL-1ra (Figure 6 and Table 1). There were slight declines in the negative ellipticity at 275−285 nm and in the positive ellipticities at 255−260 and 290−295 nm, which are the signals for tyrosine/tryptophan, phenylalanine, and tryptophan residues in the protein, respectively. The decreases in signal intensities indicate that the amino acids were positioned in a less asymmetric environment, which would indicate minor perturbations of the tertiary structure of rhIL-1ra at 37 °C.

In 0.9% (w/v) benzyl alcohol, it was not possible to monitor the changes in the phenylalanine residues as benzyl alcohol has a strong near-UV CD signal below 270 nm. However, the effects of benzyl alcohol could be monitored above this wavelength. At 25 °C, 0.9% (w/v) benzyl alcohol had minute effects on the near-UV CD spectrum for rhIL-1ra (Figure 7A and Table 1), documenting that at this temperature the tertiary structure of the protein is minimally perturbed by this preservative. At 37 °C, there was signifi-
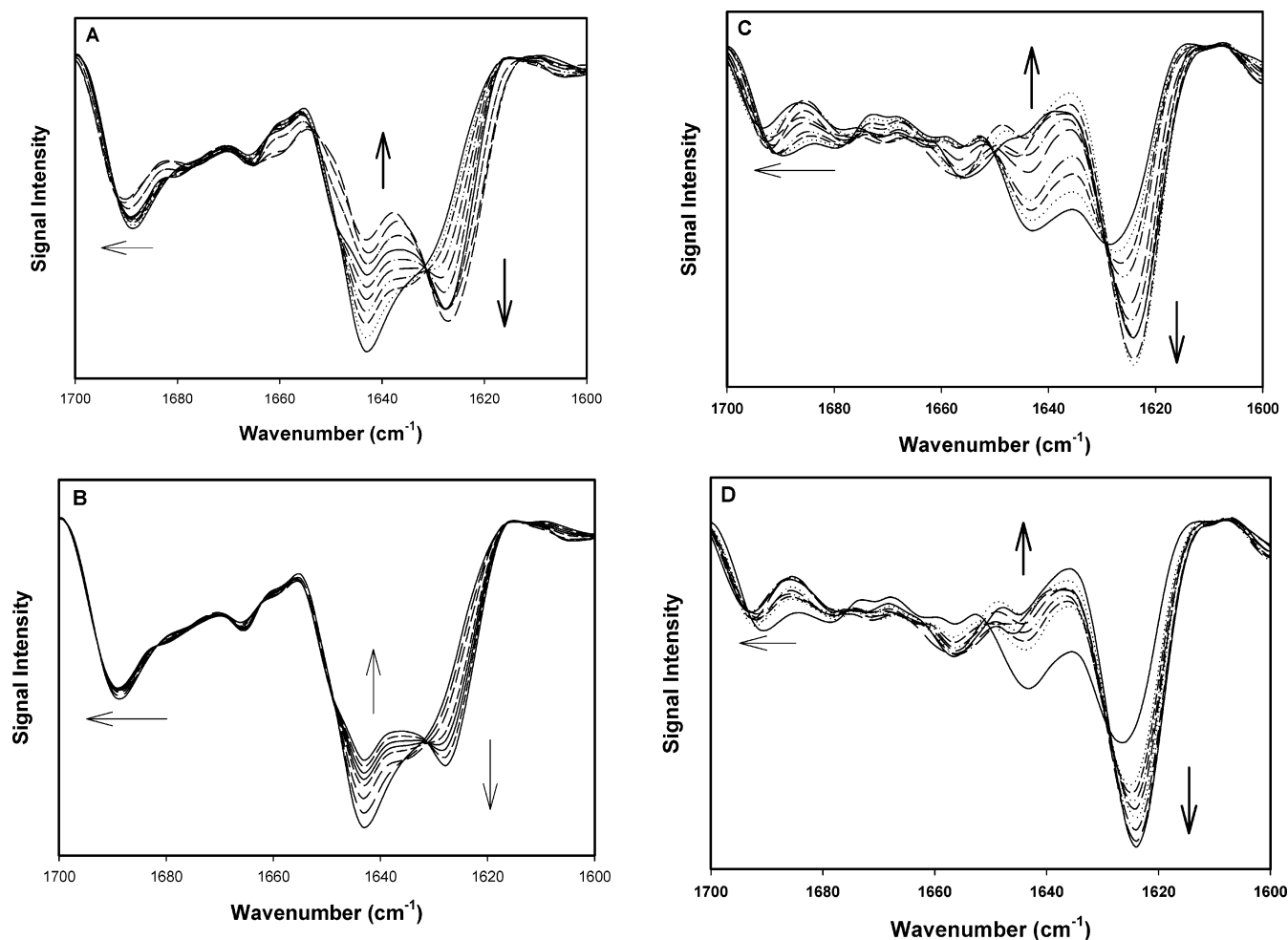
FIGURE 3: Real-time second-derivative IR spectra for rhIL-1ra in buffer alone and in the presence of benzyl alcohol or ANS at different temperatures: (A) rhIL-1ra and 0.9% (w/v) benzyl alcohol at 37 °C, (B) rhIL-1ra and 4.2 mM ANS at 37 °C, (C) rhIL-1ra and 21 mM ANS at 25 °C, and (D) rhIL-1ra and 21 mM ANS at 37 °C.

cantly greater perturbation of tertiary structure induced by 0.9% (w/v) benzyl alcohol, as evidenced by the greater decrease in the signal intensity at 275−285 nm (Figure 7B and Table 1). In contrast, in the 290−295 nm region (tryptophan signal only), no change in the ellipticity was detected in the presence of benzyl alcohol, even at the elevated temperature, compared to that for the protein in buffer alone. These results could indicate that there is a lack of structural change in the protein affecting microenvironments of the tryptophan residues. However, rhIL-1ra has two tryptophans, one of which at position 120 is substantially solvent exposed (*53*). Therefore, at 37 °C, it may be that the microenvironment of the solvent-exposed trytophan upon binding of hydrophobic benzyl alcohol will likely be akin to the protein interior. Therefore, the lack of change in the 290−295 nm region of the CD spectra could also be due to ellipticity compensation, as a consequence of protein unfolding and ligand binding occurring simultaneously.

However, overall, it can be concluded from our near-UV CD data that, at elevated temperatures, there is an increase in the population of partially unfolded protein molecules (relatively unchanged secondary structure but with an altered tertiary structure) in the presence of benzyl alcohol. We hypothesize this increase is due to a strengthening of hydrophobic interactions between benzyl alcohol and rhIL-1ra which drives the protein population toward one, which

binds more ligand at elevated temperatures according to the Wyman linkage function (*12*).

Effect of Temperature and Benzyl Alcohol on rhIL-1ra Cysteine Reactivity. The reactivity of cysteine residues in rhIL-1ra with NbdCl was used to determine the effect of temperature and benzyl alcohol on the conformational dynamics of rhIL-1ra (*26*). Native rhIL-1ra contains four free cysteine residues and no disulfide bonds (*25*). The reactivity of thiol groups with NbdCl arises because of increased solvent accessibility around the reactive cysteines when the protein molecule is expanded from its native state (*26, 49*). Therefore, the relative reaction rate is correlated directly with the time-averaged conformation of the protein.

In all cases, the cysteine reactivity profile of the protein had an initial fast phase followed by a slow phase (Figure 8A). The data were fit to an equation as explained in Materials and Methods to determine the effect of temperature and benzyl alcohol on the fast and slow reacting cysteines. An illustrative example of the fit obtained is shown in Figure 8B for rhIL-1ra with 0.9% (w/v) benzyl alcohol at 37 °C. The two phases of reactivity (Table 2) indicated the presence of two groups of reactive free cysteines in rhIL-1ra. Kendrick et al. (*26*) determined previously that the slow reacting cysteines in rhIL-1ra were residues 66 and 69 and the fast reacting cysteines were residues 116 and 122. Consistent with the relative reaction rates, the crystal structure of rhIL-1ra
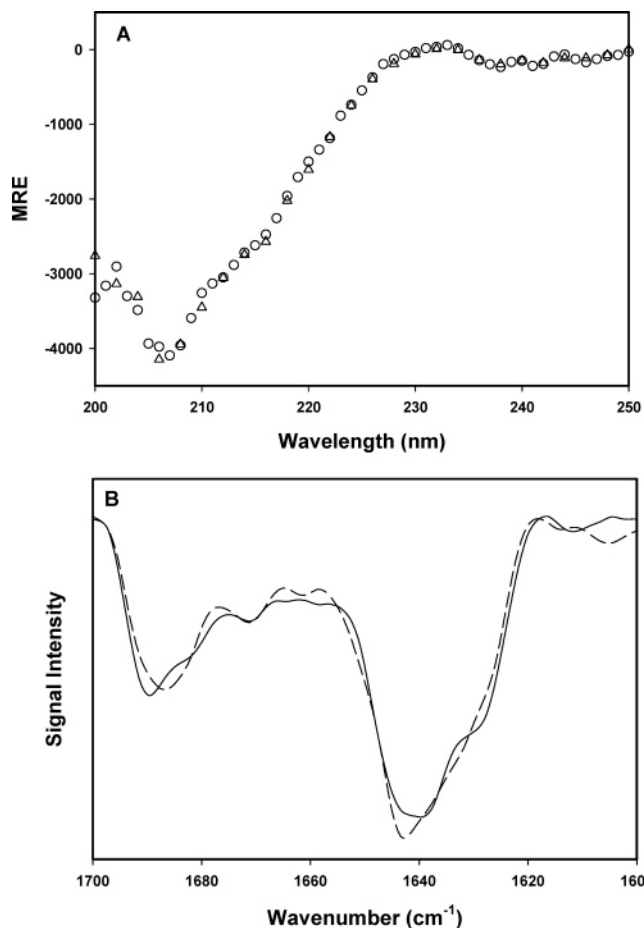
FIGURE 4: Secondary structure of rhIL-1ra in buffer alone determined as a function of temperature: (A) far-UV CD spectra at 25 (O) and 37 °C (△) and (B) IR spectra at 25 (—) and 37 °C (− − −).
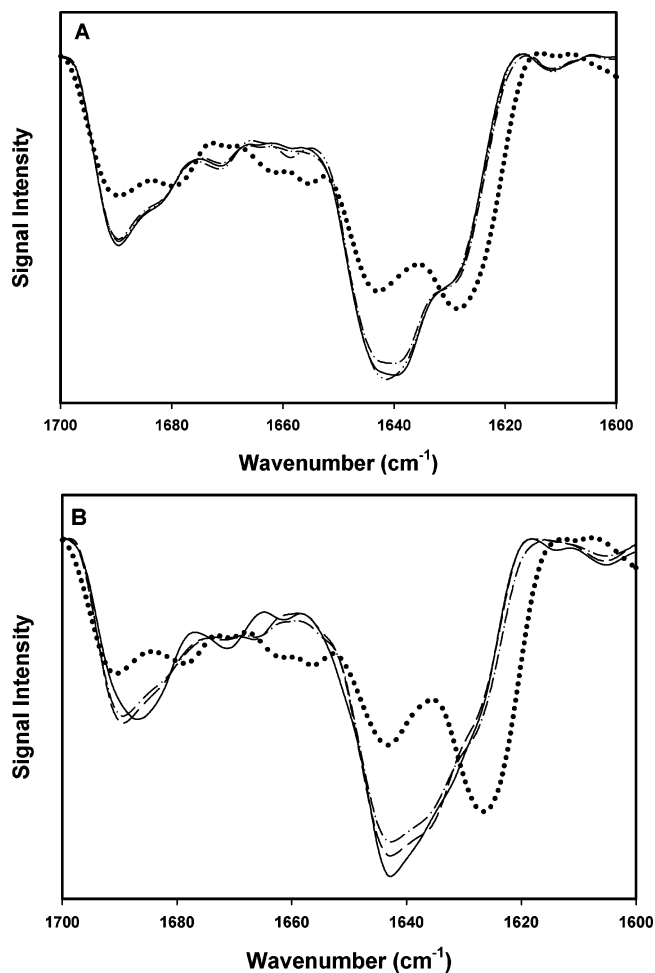

FIGURE 5: Effects of benzyl alcohol and ANS on IR spectra of rhIL-1ra at 25 (A) and 37 °C (B): rhIL-1ra in buffer alone (—), rhIL-1ra in 0.9% (w/v) benzyl alcohol (−·−), rhIL-1ra in 4.2 mM ANS (− − −), and rhIL-1ra in 21 mM ANS (···).
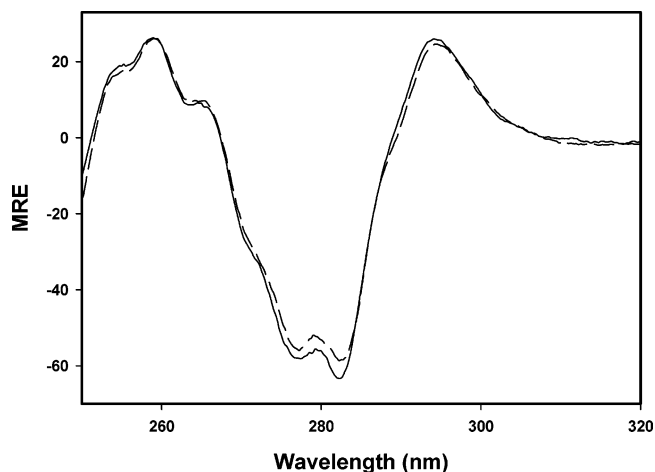

FIGURE 6: Effect of temperature on the near-UV CD spectra of rhIL-1ra in buffer alone: 25 (—) and 37 °C (− − −). Each spectrum is the average of three separate scans.

shows that cysteines 66 and 69 are in the interior of the protein and cysteines 116 and 122 are more solvent-exposed (*53*). As seen from Table 2, both increased temperature and benzyl alcohol accelerated significantly the reaction of cysteines 66 and 69 and had only minor effects on the fast reacting cysteines. For rhIL-1ra in buffer alone, there is a doubling of the reaction rate of the slow reacting cysteines upon going from 25 to 37 °C. Benzyl alcohol had little effect on the cysteine reaction rates at 25 °C but was found to significantly increase the reactivity of the slow reacting cysteines at 37 °C, compared to that of the protein in buffer alone.

The activation energies of the fast and slow reacting cysteines were determined by performing cysteine reactivity experiments over the temperature range from 20 to 42 °C. The reaction rates of the fast and slow reacting cysteines over this temperature range are listed in Table 2. From an Arrhenius plot of the natural logarithm of the fast and slow reaction rates versus the inverse of the absolute temperature (data not shown), apparent activation energies for the cysteine reactions were calculated. For the fast reacting cysteines, the apparent activation energy for the protein in buffer alone and in the presence of benzyl alcohol was around 0.25 kcal/mol, comparable to those of diffusion-limited reactions (*56–58*). In contrast, a significantly higher apparent activation energy was calculated for the slow reacting cysteines, in the range of 12 kcal/mol. The larger apparent activation energy

of the slow reacting cysteines probably is a consequence of structural perturbations in rhIL-1ra, leading to the reactivity of these buried cysteines. Thus, for solvent-exposed cysteines 116 and 122, reactivity is diffusion-limited, whereas for buried cysteines 66 and 69, structural alteration of the protein is required for reaction with NbdCl.

Table 1: Mean Residue Ellipticity at 279.25 nm for rhIL-1ra in Buffer Alone and with 0.9% (w/v) Benzyl Alcohol at Different Temperatures[a]

	25 °C	37 °C
rhIL-1ra with buffer alone	−55.6 ± 0.1	−52.3 ± 0.1
rhIL-1ra with buffer and 0.9% (w/v) benzyl alcohol	−54.4 ± 0.2	−46.5 ± 0.1
decrease in MRE with 0.9% (w/v) benzyl alcohol	1.2 ± 0.1	5.7 ± 0.1

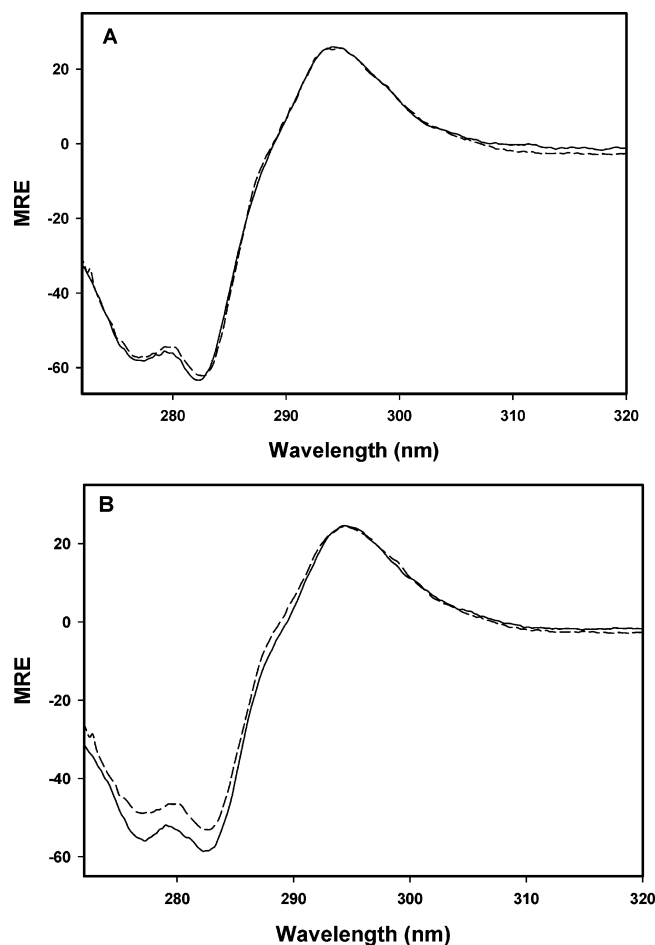[a] Values are means ± the standard deviation for triplicate samples.

FIGURE 7: Effects of 0.9% (w/v) benzyl alcohol on near-UV CD spectra of rhIL-1ra at 25 (A) and 37 °C (B): rhIL-1ra in buffer alone (—) and rhIL-1ra in 0.9% (w/v) benzyl alcohol (− − −). Each spectrum is the average of three separate scans.

Thermal Denaturation and Aggregation of rhIL-1ra. The thermal stability of rhIL-1ra in buffer alone and with 0.9% benzyl alcohol was determined using UV spectroscopy, near-UV CD, and DSC. The thermostability of rhIL-1ra in the presence of ANS was assessed using DSC due to limitations in the use of spectroscopic techniques as mentioned earlier. During the heating step, the protein aggregated irreversibly in all the solutions that were tested.

Using UV spectroscopy, a change in the tryptophan peak position and the optical density at 350 nm for rhIL-1ra in buffer alone and with 0.9% (w/v) benzyl alcohol as function of temperature were measured (Figure 9A,B). As controls, the temperature dependencies of the second-derivative UV spectra of *N*-acetyltyrosinamide and *N*-acetyltryptophanmide were assessed in the presence and absence of 0.9% (w/v) benzyl alcohol (Figure 9A). The results indicate that the
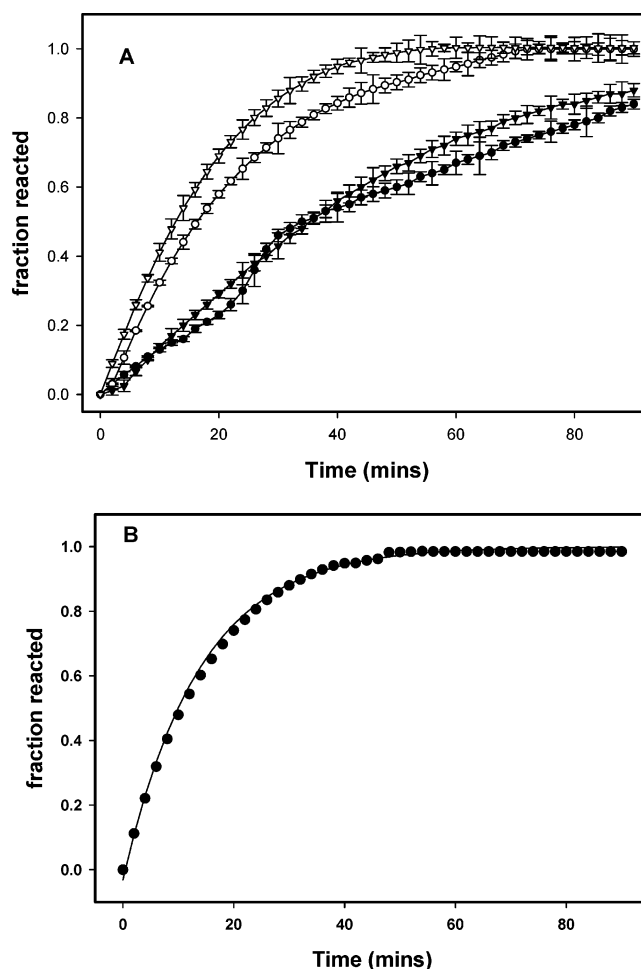

FIGURE 8: (A) Effect of temperature on the cysteine reactivity of rhIL-1a in buffer alone and with 0.9% (w/v) benzyl alcohol: rhIL-1ra in buffer alone at 25 °C (●), rhIL-1ra with benzyl alcohol at 25 °C (▼), rhIL-1ra in buffer alone at 37 °C (○), and rhIL-1ra with benzyl alcohol at 37 °C (▽). Error bars indicate the standard deviation of triplicate samples. (B) Monoexponential best fit for rhIL-1ra with benzyl alcohol at 42 °C indicated by a solid line.

Table 2: Fast and Slow Reaction Rates (min^{-1}) of rhIL-1ra Cysteines[a]

	rhIL-1ra in buffer		rhIL-1ra with 0.9% (w/v) benzyl alcohol	
temp (°C)	k_{fast} (min^{-1})	k_{slow} (min^{-1})	k_{fast} (min^{-1})	k_{slow} (min^{-1})
20	0.931 ± 0.015	0.018 ± 0.003	0.931 ± 0.013	0.019 ± 0.003
25	0.936 ± 0.010	0.021 ± 0.002	0.930 ± 0.005	0.024 ± 0.001
30	0.937 ± 0.020	0.023 ± 0.003	0.936 ± 0.013	0.025 ± 0.001
37	0.940 ± 0.029	0.048 ± 0.002	0.946 ± 0.014	0.068 ± 0.003
42	0.969 ± 0.011	0.072 ± 0.004	0.954 ± 0.017	0.095 ± 0.002

[a] Values are means ± the standard deviation for triplicate samples.

pretransition slope of the plot for the protein spectral data is due to a direct effect of temperature on aromatic residues. However, the transitions occurring in spectra of solutions containing rhIL-1ra are due to protein structural transitions. Benzyl alcohol decreased the thermostability of rhIL-1ra, as evidenced by a lower transition temperature for the tryptophan peak red shift than for the protein in buffer alone. The reduction in transition temperature is associated with benzyl alcohol-induced aggregation. Similar results were obtained when the tyroine/tryptophan peak intensity and the *a*/*b* ratio were plotted (data not shown). During thermal

Table 3: Thermodynamic Parameters for Binding of rhIL-1ra to Benzyl Alcohol

[rhIL-1ra] (mM)	[benzyl alcohol] (mM)	temp (°C)	n	K_a (M^{-1})	K_d (mM)	ΔH (kcal/mol)	ΔG (kcal/mol)	ΔS (kcal mol^{-1} K^{-1})
3	145	25	3.025 ± 0.007	90.02 ± 1.15	11.1 ± 0.14	-0.335 ± 0.007	-2.655 ± 0.007	0.0078 ± 0.00003
3	145	37	3.99 ± 0.02	88.95 ± 1.76	11.24 ± 0.22	-0.280 ± 0.007	-2.76 ± 0.014	0.0080 ± 0.00004

Table 4: Thermodynamic Parameters for Binding of rhIL-1ra to ANS

[rhIL-1ra] (mM)	[ANS] (mM)	temp (°C)	n	K_a (M^{-1})	K_d (mM)	ΔH (kcal/mol)	ΔG (kcal/mol)	ΔS (kcal mol^{-1} K^{-1})
0.735	4.2	25	1.05 ± 0.03	5499 ± 4.15	0.18 ± 0.04	-10.7 ± 0.52	-5.05 ± 0.10	-0.018 ± 0.005

[rhIL-1ra] (mM)	[ANS] (mM)	temp (°C)	n_1	K_{a1} (M^{-1})	K_{d1} (mM)	ΔH (kcal/mol)	ΔG (kcal/mol)	ΔS (kcal mol^{-1} K^{-1})
0.735	4.2	37	0.49 ± 0.01	2730 ± 2.50	0.36 ± 0.03	24.50 ± 0.45	-4.85 ± 0.09	0.094 ± 0.003

[rhIL-1ra] (mM)	[ANS] (mM)	temp (°C)	n_2	K_{a2} (M^{-1})	K_{d2} (mM)	ΔH (kcal/mol)	ΔG (kcal/mol)	ΔS (kcal mol^{-1} K^{-1})
0.735	4.2	37	0.56 ± 0.03	2760 ± 3.91	0.36 ± 0.05	-7.74 ± 0.60	-4.86 ± 0.15	-0.0092 ± 0.0007

FIGURE 10: Differential scanning microcalorimetry traces: rhIL-1ra in buffer alone (—), with benzyl alcohol (− − −), with 4.2 mM ANS (−·−), and with 21 mM ANS (−··−).
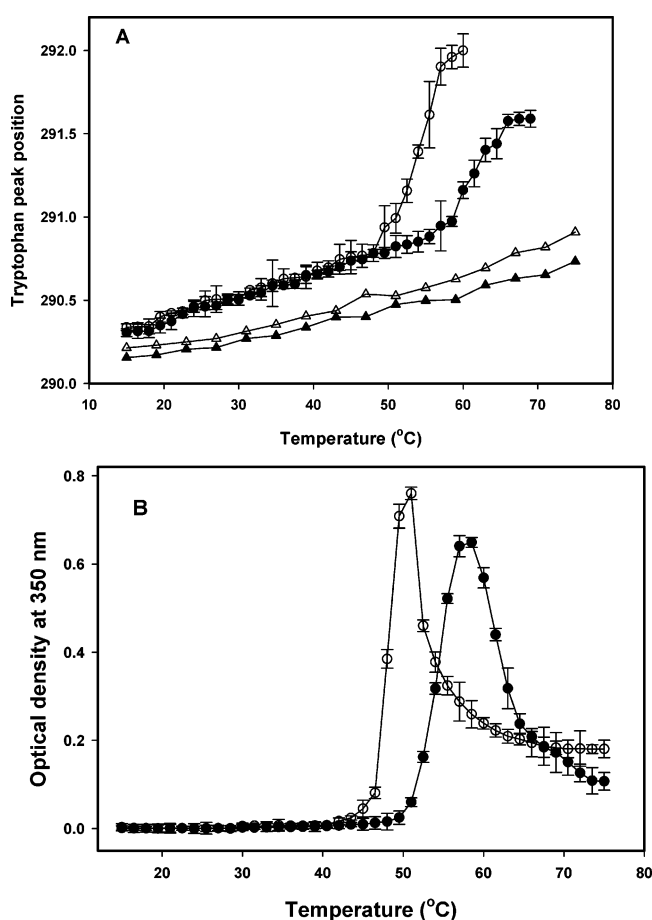
FIGURE 9: Thermal denaturation of rhIL-1ra in buffer alone and with 0.9% (w/v) benzyl alcohol using UV spectroscopy. (A) Tryptophan peak position and (B) optical density at 350 nm as a function of temperature: rhIL-1ra in buffer alone (●), rhIL-1ra and benzyl alcohol (○), and a 3:2 mixture of *N*-acetyltyrosinamide and *N*-acetyltryptophanamide in buffer alone (▲) and with benzyl alcohol (△).

All samples aggregated during the microcalorimetry experiments, thus providing only an apparent melting temperature (T_m) for the samples (Figure 10). These experiments could not be performed at a protein concentration lower than 1 mg/mL because the heat capacity change for the protein in the presence of 21 mM ANS was extremely small. For the protein in buffer alone, an apparent T_m of approximately 56 °C was measured which was lowered with 0.9% (w/v) benzyl alcohol or ANS. A decrease in the apparent T_m indicates that benzyl alcohol and ANS foster rhIL-1ra aggregation at a lower temperature.

Thermodynamics of Binding of Benzyl Alcohol and ANS to rhIL-1ra. ITC measurements for the binding of benzyl alcohol and 4.2 mM ANS to rhIL-1ra were performed at 25 and 37 °C. These measurements could not be conducted with 21 mM ANS due to aggregation of rhIL-1ra at both temperatures. Figure 11A shows representative ITC data for the titration of rhIL-1ra with benzyl alcohol at 37 °C. The enthalpy change as a function of molar ratio of benzyl alcohol to rhIL-1ra increased without a clear inflection point (Figure 11B). Using Origin supplied by Microcal, the results were best fit by employing a model with a one-type binding site model. The thermodynamic parameters are listed in Table 3. The apparent number of benzyl alcohol molecules binding

scanning, the OD$_{350}$ for rhIL-1ra in 0.9% (w/v) benzyl alcohol had an onset at 42 °C, 6 °C lower than that for rhIL-1ra in buffer alone. Results for thermal scanning monitored with near-UV CD spectroscopy also showed that 0.9% (w/v) benzyl alcohol lowered the transition temperature for rhIL-1ra (data not shown).
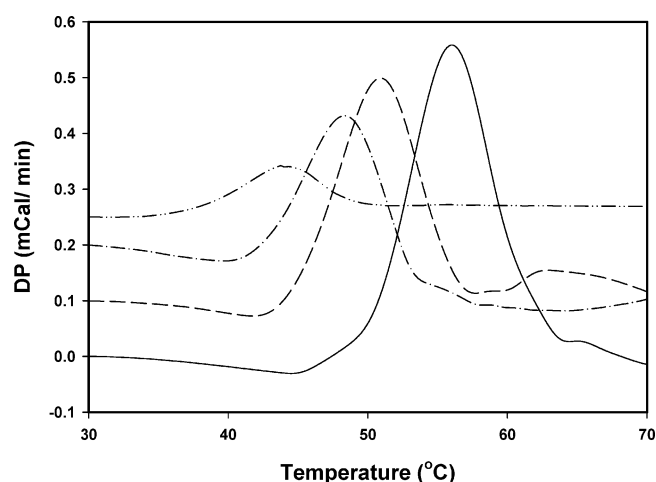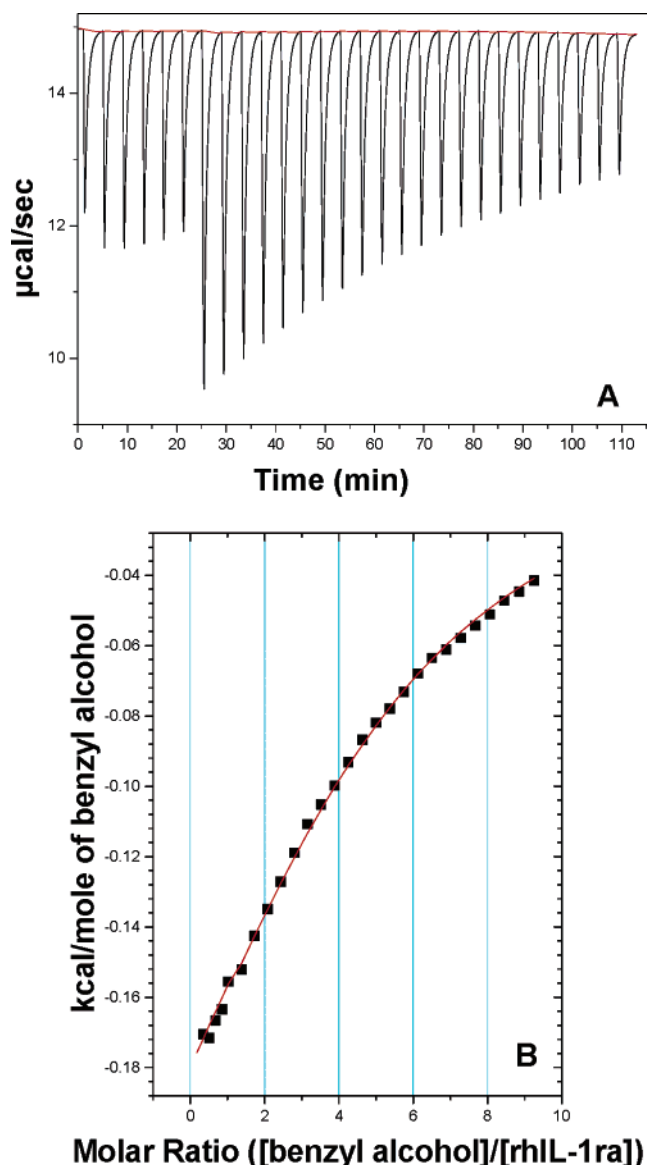
FIGURE 11: Representative ITC data for the titration of 145 mM benzyl alcohol into 3 mM rhIL-1ra at 37 °C. (A) Raw heat data as a function of injection number. (B) Enthalpy changes as a function of molar ratios of benzyl alcohol to rhIL-1ra.
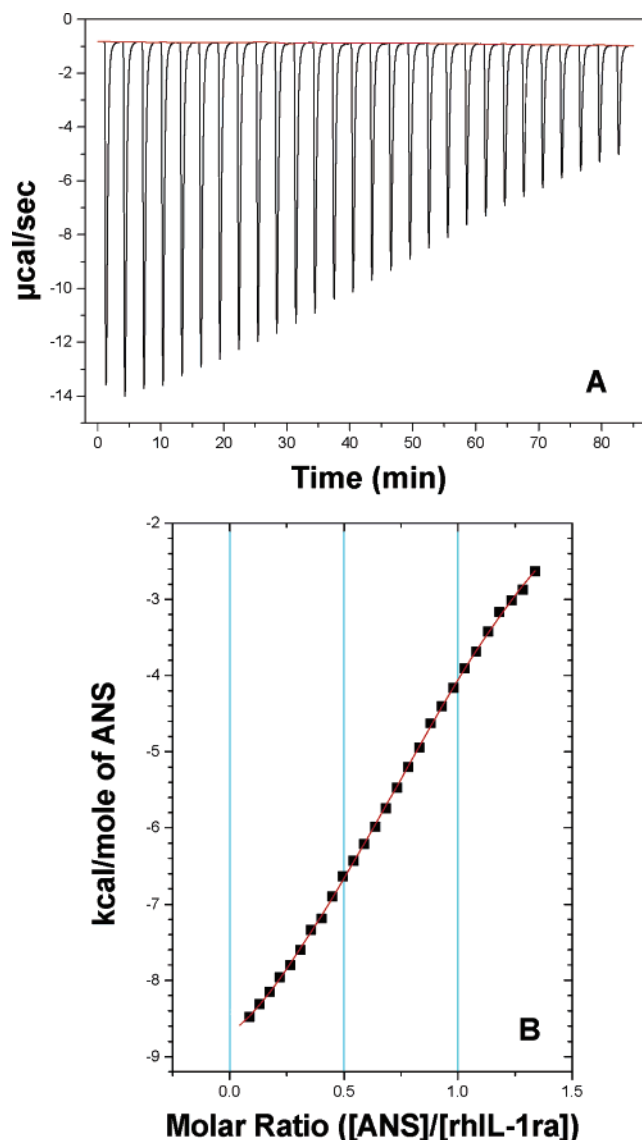

FIGURE 12: Representative ITC data for the titration of 4.2 mM ANS into 0.735 mM rhIL-1ra at 37 °C. (A) Raw heat data as a function of injection number. (B) Enthalpy changes as a function of molar ratios of ANS to rhIL-1ra.

to rhIL-1ra increased from 3.0 to 4.0 as the temperature was increased from 25 to 37 °C. The binding of benzyl alcohol to rhIL-1ra was weak even at the higher temperature as indicated by the value of the dissociation constant (K_d) in the millimolar range (*51, 59*). The free energy of interaction was almost invariant over a temperature range due to enthalpy−entropy compensation. The enthalpic contribution to the free energy of binding was small, while the entropy of binding was positive and increased with temperature, characteristic of hydrophobic interactions (*59, 60*).

It should be pointed out that the "stoichiometry" obtained for the binding of benzyl alcohol to rhIL-1ra should not be viewed as a specific interaction, because binding is occurring at relatively high concentrations of alcohol (87 mM), although some specific interactions with the solvent-exposed tryptophan may be possible as mentioned earlier. Rather, the *n* value measured here is probably a summation of many weak preferential interactions between the two species (*18*). In this context and on the basis of information obtained from

our structural studies, the small increase in *n* from 25 to 37 °C likely reflects an increase in the population of partially unfolded protein molecules with more hydrophobic surfaces. This change driven by an increased strength for hydrophobic interactions at elevated temperatures results in a greater number of weak interactions of benzyl alcohol with rhIL-1ra.

The mode of interaction of ANS with rhIL-1ra was dependent on the reaction temperature (Table 4). At 25 °C, the data were fit best with a one-type binding site model, with the interaction being predominantly enthalpic. At pH 7, the net charge on rhIL-1ra (pI 5.4) is negative. However, eight arginines and nine lysines in rhIL-1ra bear a positive charge at this pH, with pK_a's of 10 and 13, respectively (*61*), and can therefore participate in enthalpically favorable electrostatic interactions with the negatively charged sulfonate group of ANS (*35, 36, 62*). In fact, a recent study has demonstrated the presence of a highly positively charged anion-binding site on the surface of rhIL-1ra contributed by lysine 93 and lysine 96 of the 84−98 loop, as well as by

lysine 6 of the unstructured N-terminal region of residues 1−7 (63). This site could be responsible for the electrostatic interactions measured between rhIL-1ra and ANS at 25 °C.

This was not the case at 37 °C. At this temperature, the binding of ANS to rhIL-1ra was best described by a two-type binding site model, where both entropically and enthalpically favorable interactions were found to be present. The ability of ANS to induce peptide aggregation due to hydrophobic and electrostatic interactions by virtue of possessing both apolar rings and negative charges has been recently suggested (42) and was documented in the case of rhIL-1ra in this study. The binding stoichiometry between ANS and rhIL-1ra remained unchanged at the higher temperature, but a significant fraction of these interactions were found to be dominated by entropically driven hydrophobic interactions (Table 4). As noted above, the alteration in the tertiary structure of rhIL-1ra at 37 °C as seen by near-UV CD in this study probably results in an increase in the population of rhIL-1ra molecules with a greater hydrophobic exposure. This structural change, combined with the tendency of hydrophobic interactions to be strengthened at elevated temperatures, probably leads to an increase in the strength of hydrophobic interactions between ANS and rhIL-1ra molecules at 37 °C.

DISCUSSION

Effect of Temperature on Aggregation of rhIL-1ra. The purpose of this study was to understand the effect of temperature on ligand-induced protein aggregation. Two compounds, benzyl alcohol and ANS, and a model therapeutic protein rhIL-1ra were investigated. Elevated temperatures enhanced hydrophobic ligand−protein interactions but also affected the conformational and aggregation behavior of rhIL-1ra, even in the absence of such ligands. A significantly stronger protein aggregation was measured for rhIL-1ra in buffer alone at 37 °C than at 25 °C. CD spectroscopic analysis revealed that although the secondary structure of rhIL-1ra was not affected, its tertiary structure was slightly altered at the higher temperature. Cysteine reactivity experiments documented a significant increase in the reactivity of normally buried slow reacting cysteines of rhIL-1ra at the elevated temperature. Together, these results indicate an increase in the population of partially unfolded rhIL-1ra molecules as the temperature is increased from 25 to 37 °C.

The protein native molecule is not static; rather, it exists as an ensemble of native substates with different degrees of structural expansion and compaction (64). Going from 25 to 37 °C leads to an increase in the population of aggregation-prone partially unfolded protein molecules in solution. Kendrick et al. (65) has shown previously with rhIFN-γ that a structural expansion of only 9% in the protein surface area in the native state ensemble may be sufficient to induce protein aggregation. Similarly, in this study, even though a small change in the tertiary structure was observed at 37 °C, it was sufficient to induce significant protein aggregation. However, it is unclear whether aggregation of rhIL-1ra proceeds due to weak partial unfolding of all protein molecules in solution or through greater unfolding of a small fraction of the population. The average nature of the spectroscopic measurements cannot differentiate between these two situations.

Effect of Temperature on Benzyl Alcohol-Induced Aggregation of rhIL-1ra. Much more rapid aggregation of rhIL-1ra in the presence of benzyl alcohol was measured at 37 °C than at 25 °C, in support of our hypothesis. Spectroscopic results documented that with benzyl alcohol, there was a greater increase in the population of partially unfolded rhIL-1ra molecules (native secondary but altered tertiary structure) at 37 °C than at 25 °C. Consistent with these results were the increase in the reactivity of the buried cysteines caused by benzyl alcohol at 37 °C and a lack of this effect at 25 °C. These data demonstrate the importance of temperature in modulating ligand−protein interactions and the resulting ligand-induced shifts in the protein population toward partially unfolded, aggregation-prone species.

Our ITC results for the interaction of benzyl alcohol and rhIL-1ra, although qualitative, do establish that there was a greater hydrophobic interaction between the two species at the higher temperature (21). This is reflected as an increase in the stoichiometry of binding for benzyl alcohol and rhIL-1ra at 37 °C compared to that at 25 °C. The enhanced hydrophobic interactions at 37 °C, via the Wyman linkage function (12), will favor the increase in the level of partially unfolded protein molecules that accounts for the greatly enhanced protein aggregation rate at 37 °C compared to that at 25 °C.

Effect of Temperature on ANS-Induced Aggregation of rhIL-1ra. In further support of our hypothesis, a strong direct temperature dependency in ANS-induced aggregation of rhIL-1ra was observed. However, the mode of interaction of ANS with rhIL-1ra was different from that of benzyl alcohol. With ANS there was a temperature-modulated switch in the thermodynamics of the interaction of ANS with the protein. At 25 °C, enthalpically favorable electrostatic interactions were dominant. At 37 °C, a significant fraction of ANS molecules interacted with the protein through entropically favorable hydrophobic interactions.

In the presence of ANS, most optical spectroscopic techniques could not be used, but IR spectroscopy did document that at 25 °C 4.2 mM ANS did not affect the protein's secondary structure whereas at 37 °C there were minor alterations in secondary structure. Presumably, these spectroscopic changes reflected ANS-induced shifts in the molecular population of rhIL-1ra molecules toward partially unfolded species. Direct confirmation of this conclusion by investigation of protein tertiary structural changes could not be obtained due to the interference of ANS with the optical spectroscopic methods employed in this study.

At 21 mM ANS, rapid aggregation of rhIL-1ra was observed even at 25 °C. In contrast, in 4.2 mM ANS at 25 °C, aggregation was not accelerated. A similar concentration-dependent effect of bis-ANS has been seen with oligomerization of a full-length prion protein (43) and was attributed to hydrophobic interactions between the two species at higher bis-ANS concentrations. Our study underscores that a critical determinant of ANS-induced protein aggregation is whether enough hydrophobic interactions exist to populate a sufficient level of aggregation-prone species, by using either a high concentration of ANS (21 mM) at 25 °C or elevated temperatures at a lower concentration of ANS (4.2 mM).

Furthermore, these results show that ANS is not just a "neutral probe" for partially unfolded protein molecules. Rather, because this ligand interacts more favorably with

partially unfolded protein molecules, the Wyman linkage function (*12*) predicts that the population equilibrium will be shifted toward this species in the presence of ANS. Whether this shift results in protein aggregation depends on many factors, including protein concentration, ANS concentration, and temperature.

CONCLUSIONS

The results from this study documented a strong effect of temperature on benzyl alcohol- and ANS-induced protein aggregation. Such temperature dependency, in addition to being important in improving our understanding of the fundamentals of protein−ligand interactions, could have serious practical implications. For example, multidose therapeutic protein formulations containing benzyl alcohol would usually be stored at 4−8 °C, or perhaps at room temperature after reconstitution of a dried product with water containing 0.9% benzyl alcohol. However, many investigations of protein formulation stability are performed at elevated temperatures (e.g., 37 °C) to reduce the time needed to complete a study. Because of the strong temperature dependency of benzyl alcohol-induced protein aggregation, results from the higher-temperature studies may provide results that are not predictive of what happens at actual product storage temperatures. As a result, an acceptable formulation choice may be discarded unnecessarily. Similarly, in vitro screening of ligands to identify compounds to inhibit amyloid fibril formation is sometimes performed at room temperature. Compounds that are effective at this temperature may not work as well, or perhaps could even foster protein aggregation, at a physiological temperature of 37 °C. Thus, in general, it is important to study effects of ligands on protein aggregation at the actual temperature at which the protein will be stored or functioning.

REFERENCES

1. Agorogiannis, E. I., Agorogianni, G. I., Papadimitriou, A., and Hadjigeorgiou, G. M. (2004) Protein misfolding in neurodegenerative diseases, *Neuropathol. Appl. Neurobiol. 30*, 215−224.
2. Kelly, J. W. (1996) Alternative conformations of amyloidogenic proteins govern their behavior, *Curr. Opin. Struct. Biol. 6*, 11−17.
3. Serpell, L. C., Sunde, M., and Blake, C. C. (1997) The molecular basis of amyloidosis, *Cell. Mol. Life Sci. 53*, 871−887.
4. Moore, W. V., and Leppert, P. (1980) Role of aggregated growth hormone in development of antibodies to hGH, *J. Clin. Endocrinol. Metab. 4*, 691−697.
5. Ratner, R. E., Phillips, T. M., and Steiner, M. (1990) Persistent cutaneous insulin allergy resulting from high molecular weight insulin aggregates, *Diabetes 39*, 728−733.
6. Thornton, C. A., and Ballow, M. (1993) Safety of intravenous immunoglobulin, *Arch. Neurol. 50*, 135−136.
7. Fink, A. L. (1998) Protein aggregation: Folding aggregates, inclusion bodies and amyloid, *Folding Des. 3*, 9−23.
8. Kendrick, B. S., Carpenter, J. F., Cleland, J. L., and Randolph, T. W. (1998) A transient expansion of the native state precedes aggregation of recombinant human interferon-γ, *Proc. Natl. Acad. Sci. U.S.A. 95*, 14142−14146.
9. Kendrick, B. S., Cleland, J. L., Lam, X., Nguyen, T., Randolph, T. W., Manning, M. C., and Carpenter, J. F. (1998) Aggregation of recombinant human interferon γ: Kinetics and structural transitions, *J. Pharm. Sci. 87*, 1069−1076.
10. Petrassi, H. M., Johnson, S. M., Purkey, H. E., Chiang, K. P., Walkup, T., Jiang, X., Powers, E. T., and Kelly, J. W. (2005) Potent and selective structure-based dibenzofuran inhibitors of transthyretin amyloidogenesis: Kinetic stabilization of the native state, *J. Am. Chem. Soc. 127*, 6662−6671.
11. Jackson-Booth, P. G., Terry, C., Lackey, B., Lopacynzka, M., and Nissley, P. (2003) Inhibition of the biologic response to insulin-like growth factor I in MCF-7 breast cancer cells by a new monoclonal antibody to the insulin-like growth factor-I receptor. The importance of receptor down-regulation, *Horm. Metab. Res. 3*, 850−856.
12. Timasheff, S. N. (1998) Control of protein stability and reactions by weakly interacting cosolvents: The simplicity of the complicated, *Adv. Protein Chem. 51*, 342−355.
13. Wiseman, R. L., Johnson, S. M., Kelker, M. S., Foss, T., Wilson, I. A., and Kelly, J. W. (2005) Kinetic stabilization of an oligomeric protein by a single ligand binding event, *J. Am. Chem. Soc. 127*, 5540−5551.
14. Tsai, P. K., Volkin, D. B., Dabora, J. M., Thompson, K. C., Bruner, M. W., Gren, J. O., Matuszewska, B., Keogan, M., Boudi, J. W., and Middaugh, C. R. (1993) Formulation design of acidic fibroblast growth factor, *Pharm. Res. 5*, 649−659.
15. Volkin, D. B., Tsai, P. K., Dabora, J. M., Gress, J. O., Burke, C. J., Linhardt, R. J., and Middaugh, C. R (1993) Physical stabilization of acidic fibroblast growth factor by polyanions, *Arch. Biochem. Biophys. 300*, 30−41.
16. Kim, Y. S., Randolph, T. W., Manning, M. C., Stevens, F. J., and Carpenter, J. F. (2003) Congo red populates partially unfolded states of an amyloidogenic protein to enhance aggregation and amyloid fibril formation, *J. Biol. Chem. 278*, 10842−10850.
17. Cordeiro, Y., Machado, F., Juliano, L., Juliano, M. A., Brentani, R. R., Foguel, D., and Silva, J. L. (2001) DNA converts cellular prion proteins into the β sheet conformation and inhibits peptide aggregation, *J. Biol. Chem. 52*, 49400−49409.
18. Zhang, Y., Roy, S., Jones, L. S., Krishnan, S., Kerwin, B. A., Chang, B. S., Manning, M. C., Randolph, T. W., and Carpenter, J. F. (2004) Mechanism for benzyl alcohol-induced aggregation of recombinant human interleukin-1 receptor antagonist in aqueous solution, *J. Pharm. Sci. 93*, 3076−3089.
19. Hetenyi, C., Szabo, Z., Klement, E., Datki, Z., and Kortvelyesi, T. (2002) Pentapeptide amides interfere with the aggregation of β-amyloid peptide of Alzheimer's disease, *Biochem. Biophys. Res. Commun. 292*, 931−936.
20. Chang, B. S., and Hershenson, S. (2002) in *Rational design of stable protein formulations: Theory and Practice* (Carpenter, J. F., and Manning, M. C., Eds.) pp 1−25, Kluwer Academic/Plenum Publishers, New York.
21. Dill, K. A. (1990) Dominant forces in protein folding, *Biochemistry 29*, 7133−7155.
22. Arakawa, T., Carpenter, J. F., Kita, Y. A., and Crowe, J. H. (1990) The basis for toxicity of certain cryoprotectants: A hypothesis, *Cryobiology 27*, 401−415.
23. Fink, A. (1995) Compact intermediate states in protein folding, *Annu. Rev. Biophys. Biomol. Struct. 24*, 495−522.
24. Ptitsyn, O. B., Pain, R. H., Semistonov, G. V., Zerovnik, E., and Razgulyaev, O. I. (1990) Evidence of a molten globule state as a general intermediate in protein folding, *FEBS Lett. 262*, 20−24.
25. Chang, B. S., Reeder, G., and Carpenter, J. F. (1996) Development of a stable freeze-dried formulation of recombinant human interleukin-1 receptor antagonist, *Pharm. Res. 13*, 242−249.
26. Kendrick, B. S., Chang, B. S., Arakawa, T., Peterson, B., Randolph, T. W., Manning, M. C., and Carpenter, J. F. (1997) Preferential exclusion of sucrose from recombinant interleukin-1 receptor antagonist: Role in restricted conformational mobility and compaction of native state, *Proc. Natl. Acad. Sci. U.S.A. 94*, 11917−11922.
27. Roy, S., Jung, R., Kerwin, B. A., Randolph, T. W., and Carpenter, J. F. (2005) Effects of benzyl alcohol on aggregation of recombinant human interleukin-1-receptor antagonist in reconstituted lyophilized formulations, *J. Pharm. Sci. 94*, 382−396.
28. Akers, M. J. (1984) Considerations in selecting antimicrobial agents for parenteral product development, *Pharm. Technol. 8*, 36−46.
29. Maa, Y. F., and Hsu, C. C. (1996) Aggregation of recombinant human growth hormone induced by phenolic cmpounds, *Int. J. Pharm. 140*, 155−168.
30. Lam, X., Papatoff, T. W., and Nguyen, T. H. (1997) The effect of benzyl alcohol on recombinant human interferon-γ, *Pharm. Res. 14*, 725−729.
31. Ramboraina, S., and Redfield, C. (2003) Structural characterisation of the human α-lactalbumin molten globule at high temperature, *J. Mol. Biol. 330*, 1177−1188.

32. Sehorn, M. G., Slepenkov, S. V., and Witt, S. N. (2002) Characterization of Two Partially Unfolded Intermediates of the Molecular Chaperone DnaK at Low pH, *Biochemistry 41*, 8499−8507.

33. Matulis, D., and Lovrien, R. (1998) 1-Anilino-8-naphthalene sulfonate anion-protein binding depends primarily on ion pair formation, *Biophys. J. 74*, 422−429.

34. Ali, V., Koodathingal, P., Kulkarni, S., Ahmad, A., Madhusudan, K. P., and Bhakuni, B. (1999) 8-Anilino-1-naphthalene sulfonic acid (ANS) induces folding of acid unfolded cytochrome *c* to molten globule state as a result of electrostatic interactions, *Biochemistry 38*, 13635−13642.

35. Matulis, D., Baumann, C. G., Bloomfield, V. A., and Lovrien, R. E. (1999) 1-Anilino-8-naphthalene sulfonate as a protein conformational tightening agent, *Biopolymers 49*, 451−458.

36. Kumar, M. S., Kapoor, M., Sinha, S., and Reddy, G. B. (2005) Insights into hydrophobicity and the chaperone-like function of αA- and αB-crystallins: An isothermal titration calorimetric study, *J. Biol. Chem. 280*, 21726−21730.

37. Gibbons, D. L., and Horowitz, P. M. (1995) Exposure of hydrophobic surfaces on the chaperonin GroEL oligomer by protonation or modification of His-401, *J. Biol. Chem. 270*, 7335−7340.

38. Stevens, A., and Augusteyn, R. C. (1997) Binding of 1-anilinon-aphthalene-8-sulfonic acid to α-crystallin, *Eur. J. Biochem. 243*, 792−797.

39. Ferraro Gonzales, A. D., Palmieri, L., Valory, M., Silva, J. L., Lashuel, H., Kelly, J. W., and Foguel, D. (2003) Hydration and packing are crucial to amyloidogenesis as revealed by pressure studies on transthyretin variants that either protect or worsen amyloid disease, *J. Mol. Biol. 328*, 963−974.

40. Itzhaki, L. S., Evans, P. A., Dobson, C. M., and Radford, S. E. (1994) Tertiary interactions in the folding of hen lysozyme: Kinetic studies using fluorescent probes, *Biochemistry 33*, 5212−5220.

41. Engelhard, M., and Evans, P. A. (1995) Kinetics of interaction of partially folded proteins with a hydrophobic dye: Evidence that molten globule character is maximal in early folding intermediates, *Protein Sci. 4*, 1553−1562.

42. Ferraro-Gonzalez, A. D., Robbs, B. K., Moreau, V. H., Ferreira, A., Neto, J. L., Valente, A. P., Almeida, F. C. L., Silva, J. L., and Foguel, D. (2005) Controlling β-Amyloid Oligomerization by the Use of Naphthalene Sulfonates: TRAPPING LOW MOLECULAR WEIGHT OLIGOMERIC SPECIES, *J. Biol. Chem. 280*, 34747−34754.

43. Cordiero, Y., Lima, L. M. T. R., Gomes, M. P. B., and Foguel, D. (2003) Modulation of prion protein oligomerization, aggregation, and β-sheet conversion by 4,4′-dianilino-1,1′-binaphthyl-5,5′-sulfonate (bis-ANS), *J. Biol. Chem. 7*, 5346−5352.

44. Dobryszycki, P., Kolodziejczyk, R., Krowarcsh, D., Gapinski, J., Ozyhar, A., and Kochman, M. (2004) Unfolding and refolding of juvenile hormone binding protein, *Biophys. J. 86*, 1138−1148.

45. Fuertes, M. A., Beberich, C., Lozano, R. M., Gallego, G. G., and Alonso, C. (1999) Folding stability of the kinetoplastid membrane protein-11 (KMP-11) from *Leishmania infantum*, *Eur. J. Biochem. 260*, 559−567.

46. Zhou, H. W., Park, Y. D., and Zhou, H. M. (2002) Lead ion effect on creatine kinase: Equilibrium and kinetic studies of inactivation and conformational changes, *Int. J. Biochem. Cell Biol. 34*, 564−571.

47. Dong, A., Huang, P., and Caughey, W. S. (1990) Protein secondary structures in water from second-derivative amide I infrared spectra, *Biochemistry 29*, 3303−3308.

48. Strickland, E. H. (1974) Aromatic contributions to circular dichroism spectra of proteins, *CRC Crit. Rev. Biochem. 2*, 113−175.

49. Yancey, P. H., and Somero, G. N. (1979) Counteraction of urea destabilization of protein structure by methylamine osmoregulatory compounds of elasmobranch fishes, *Biochem. J. 183*, 317−323.

50. Ramachandran, S., Bhadresh, R. R., and Udgaonkar, J. B. (2000) Measurements of cysteine reactivity during protein unfolding suggest the presence of competing pathways, *J. Mol. Biol. 297*, 733−745.

51. Wiseman, T., Williston, S., Brandts, J. F., and Lin, L. N. (1989) Rapid measurement of binding constants and heats of binding using a new titration calorimeter, *Anal. Biochem. 179*, 131−137.

52. Dong, A., and Caughey, W. S. (1994) Infrared methods for study of hemoglobin reactions and structures, *Methods Enzymol. 232*, 139−175.

53. Stockman, B. J., Scahill, T. A., Roy, M., Ulrich, E. L., Strakalaitis, N. A., Brunne, D. P., Yem, A. W., and Deibel, M. R. (1992) Secondary structure and topology of interleukin-1 receptor antagonist protein determined by heteronuclear three-dimensional NMR spectroscopy, *Biochemistry 31*, 5237−5245.

54. Dong, A., Prestrelski, S. J., Allison, S. D., and Carpenter, J. F. (1995) Infrared spectroscopic studies of lyophilization- and temperature-induced protein aggregation, *J. Pharm. Sci. 84*, 415−424.

55. Kim, Y. S., Wall, J. S., Chi, E., Raffen, R., Wilkins-Stevens, P., Steven, F. J., Manning, M. C., Randolph, T. W., Solomon, A., and Carpenter, J. F. (2001) Counteracting effects of renal solutes on amyloid fibril formation by immunoglobulin light chains, *J. Biol. Chem. 276*, 1626−1633.

56. Lohman, T. M. (1986) Kinetics of protein-nucleic acid interactions: Use of salt effects to probe mechanisms of interaction, *CRC Crit. Rev. Biochem. 19*, 191−245.

57. Talavera, M. A., and De La Cruz, E. M. (2005) Equilibrium and kinetic analysis of nucleotide binding to the DEAD-Box RNA Helicase DbpA, *Biochemistry 44*, 959−970.

58. Abreu, M. S. C., Estronca, L. M. B. B., Moreno, M. J., and Vaz, W. L. C. (2003) Binding of a fluorescent lipid amphiphile to albumin and its transfer to lipid bilayer membranes, *Biophys. J. 84*, 386−399.

59. Holdgate, G. A. (2001) Making cool drugs hot: Isothermal titration calorimetry as a tool to study binding energetics, *Biotechnology 31*, 164−184.

60. Bijma, K., Rank, E., and Engberts, J. B. F. N. (1998) Effect of Counterion Structure on Micellar Growth of Alkylpyridinium Surfactants in Aqueous Solution, *J. Colloid Interface Sci. 205*, 245−246.

61. Branden, C., and Tooze, J. (1999) in *Introduction to Protein Structure*, Garland Publishing, New York.

62. Kundu, B., and Guptasarma, P. (1999) Hydrophobic dye inhibits aggregation of molten carbonic anhydrase during thermal unfolding and refolding, *Proteins: Struct., Funct., Genet. 37*, 321−324.

63. Raibekas, A. A., Bures, E. J., Siska, C. C., Kohno, T., Latypov, R. F., and Kerwin, B. A. (2005) Anion binding and controlled aggregation of human interleukin-1 receptor antagonist, *Biochemistry 44*, 9871−9879.

64. Wang, A., Robertson, A. D., and Bolen, D. W. (1995) Effects of a naturally occurring compatible osmolyte on the internal dynamics of ribonuclease A, *Biochemistry 34*, 15096−15104.

65. Kendrick, B. S., Carpenter, J. F., Cleland, J. L., and Randolph, T. W. (1998) A transient expansion of the native state precedes aggregation of recombinant human interferon-γ, *Proc. Natl. Acad. Sci. U.S.A. 95*, 14142−14146.